Supramolecular Chemistry
Publication details, including instructions for authors and subscription information:
http://www.informaworld.com/smpp/title~content=t713649759

Cation Coordination of Bisamidopyridine-derived Receptors as Investigated in the Solid-state and in Solution

Julia L. Bricks[a]; Günter Reck[b]; Knut Rurack[b]; Burkhard Schulz[b]; Monika Spieles[b]
[a] Institute of Organic Chemistry, Kiev, Ukraine [b] Bundesanstalt für Materialforschung und -prüfung (BAM), Berlin, Germany

Online publication date: 13 May 2010

To cite this Article Bricks, Julia L. , Reck, Günter , Rurack, Knut , Schulz, Burkhard and Spieles, Monika(2003) 'Cation Coordination of Bisamidopyridine-derived Receptors as Investigated in the Solid-state and in Solution', Supramolecular Chemistry, 15: 3, 189 — 197
To link to this Article: DOI: 10.1080/1061027031000078239
URL: http://dx.doi.org/10.1080/1061027031000078239

Supramolecular Chemistry, 2003 Vol. 15 (3), pp. 189–197

Cation Coordination of Bisamidopyridine-derived Receptors as Investigated in the Solid-state and in Solution

JULIA L. BRICKS[a], GÜNTER RECK[b], KNUT RURACK[b,*], BURKHARD SCHULZ[b] and MONIKA SPIELES[b]

[a]*Institute of Organic Chemistry, National Academy of Sciences of the Ukraine, Murmanskaya 5, 253660, Kiev-94, Ukraine;* [b]*Bundesanstalt für Materialforschung und -prüfung (BAM), Richard-Willstätter-Str. 11, D-12489 Berlin, Germany*

Received (in Southampton, UK) 6 September 2002; Accepted 1 October 2002

A bisamidopyridine-type receptor, *N*,*N*′-bis(6-methyl-2-pyridyl)pyridine-2,6-dicarboxamide (1), and its Co^{III} complex were prepared and their X-ray structures were compared to those of *N*,*N*′-diphenylpyridine-2,6-dicarboxamide (2) and $Co^{III}(2)_2$. Introduction of the two additional coordinative groups resulted in second-order interactions between the central ion and the nitrogen atoms of the terminal pyridine moieties in the crystalline state. Solution studies in acetonitrile revealed the importance of these interactions for the ligand's metal ion recognition ability. Whereas 2 only binds to Pb^{II} and Cu^{II}, 1 yields complexes with a majority of the heavy and transition metal ions studied, Co^{II}, Ni^{II}, Cu^{II}, Zn^{II}, Fe^{III}, Fe^{II}, Hg^{II}, and Pb^{II}, respectively. The cation binding properties in solution were investigated by absorption spectroscopy and in the case of $1–M^{II/III}$, the formation of two spectroscopically distinguishable types of complexes was found. Protonation experiments and theoretical considerations helped to gain further insight into possible modes of coordination in solution.

Keywords: Pyridine carboxamides; Ion recognition; Crystal structure; *N*-coordination

INTRODUCTION

Structural analogues of pyridine-2,6-dicarboxamide play an important role in bioinorganic and analytical chemistry. Various oxygen-activating enzymes contain transition metal ions, most prominently Fe^{III} and Co^{III}, at their reactive centers, often bound via the nitrogen atom(s) of such ligating motifs [1,2]. Besides redox and spin-state control of central ions in complexes of this type [3], in general, the coordination chemistry of carboxamido nitrogen atoms [4] is of considerable interest in bioinorganic research as it allows the study of some of the aspects of metal ion trafficking or structure–function relationships [5,6]. On the other hand, concerning analytical chemistry, bisamidopyridines and related compounds are frequently used as binding motifs in anion receptors [7–9] and for the recognition of organic molecules such as sugars [10,11], amino acids [12], or other organic compounds [13,14]. Furthermore, such functional subunits can yield hydrogen bond-stabilized supramolecular architectures [15,16].

In metal ion coordination chemistry, the central element of bisamidopyridino ligands is the planarity of the core chelating structure, the RNH–CO–pyridine–CO–NHR fragment, able to form tridentate chelates with two five-membered rings (Scheme 1). Accordingly, as the modular synthesis of such ligands with respect to the nature of substituent R is rather straightforward, a lot of effort has recently been directed towards the design of bisamidopyridino ligands with additional coordination sites at these terminal groups [3,17–20].

As an extension of our work on metal ion responsive molecular sensors [21,22], we are interested in the development and integration of new receptor subunits in various types of chromo- and fluorogenic probes. Besides exploring the possibilities of crown ether-derived chemistry [23,24], we are currently also targeting open chain receptor frameworks [25]. In this respect, a particularly interesting feature of the bisamidopyridino fragment is its versatility for integration into a chromophoric system. For instance, because signal generation relies on the interaction of a bound species such as a metal ion with a heterocyclic (donor) atom participating in

*Corresponding author: Fax: +49-30-8104-5005. E-mail: knut.rurack@bam.de

ISSN 1061-0278 print/ISSN 1029-0478 online © 2003 Taylor & Francis Ltd
DOI: 10.1080/1061027031000078239

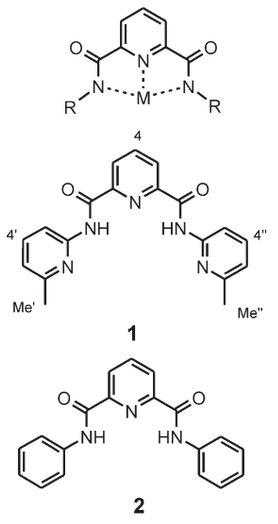

3 : Co^{III} complex of $\mathbf{1}^{2-}$ $[Co^{III}(\mathbf{1})_2]$

4 : Co^{III} complex of $\mathbf{2}^{2-}$ $[Co^{III}(\mathbf{2})_2]$

SCHEME 1 Typical structure of pyridine-2,6-dicarboxamid(at)e complexes and chemical structures of **1**–**4**. Labels 4, 4′, 4″, Me′, and Me″ denote possible sites of coupling of the ligand to a chromophoric π-system.

the probe's π-system, a suitable coordination site for triggering an ion-induced signal consists of a *para* or *ortho* substituted pyridine moiety (Scheme 1) [26]. On this basis, we prepared ligand **1**. In view of the highly topical issue that such ligands represent in the field of bioinorganic chemistry, we also synthesized the Co^{III} complex of deprotonated **1** and, for a better comparison of the effect of the two additional donor sites, the phenyl analogue **2** and its respective Co^{III} complex. The synthesis of **1**, as well as of the latter two compounds, has also been carried out previously by other groups [27–29]. In the present account, we report on the metal ion coordination chemistry of both ligands in the neutral and deprotonated state as determined by X-ray structure analysis and solution-based optical spectroscopy.

EXPERIMENTAL

For the spectroscopic studies, metal perchlorates of the highest purity available were purchased from Merck, Acros, and Aldrich and dried in a vacuum oven before use (for details, see [30]). (**Caution**: perchlorate salts present a potential explosion hazard and should be handled with care and possibly only in small quantities!) Acetonitrile from Aldrich was of UV spectroscopic grade. The purity of the synthesized compounds was checked by reversed phase HPLC (HPLC set up from Merck-Hitachi; RP18 column; acetonitrile–water = 75 : 25 as eluent) employing UV detection (UV detector from Knaur; fixed wavelength at 310 nm). The melting points were measured with a digital melting point analyser IA 9100 (Kleinfeld GmbH) and are uncorrected. NMR spectra were obtained with a 500 MHz NMR spectrometer Varian $Unity_{plus}$ 500 and the mass spectrum of **1** was recorded on a MAT 95 spectrometer with API-II (Finnigan MAT, Bremen).

The X-ray data of **1**, **3**, and **4** were collected on a Bruker AXS SMART diffractometer equipped with a CCD area detector. The structures were solved by direct methods and refined by full-matrix least-squares calculations using SHELX-97 [31]. The hydrogen atoms of all the structures were introduced in their calculated positions and refined using riding models. The relatively high *R* value for **3** is caused by the poor quality of the available single crystals and statistical disorder phenomena of many water molecules. Atomic coordinates, thermal parameters, and bond lengths and angles (CIF files) have been deposited at the Cambridge Crystallographic Data Centre (CCDC) and allocated the deposition numbers CCDC 192575 (**1**), CCDC 192576 (**3**), and CCDC 192574 (**4**). It should be noted that our results on **1** and **2** are in good agreement with previous reports [29,32].

The optical spectra were recorded on Bruins Instruments Omega 10 and Perkin–Elmer Lambda 9 spectrophotometers. For further details on absorption measurements, see [30]. The complex stability constants reported here were determined from spectrophotometric titrations in 10 mm absorption cells and with a ligand concentration of 5×10^{-6} M. The data were fitted to models introduced by Valeur *et al.* [33,34], or by employing Hill-type analyses with the program package Origin V7.0, OriginLab Corporation.

N,*N*′-Bis(6-methyl-2-pyridyl)pyridine-2,6-dicarboxamide (1)

Pyridine-2,6-dicarboxylic acid (3.0 g, 18 mmol) was suspended in pyridine (10 ml). 2-Amino-6-methylpyridine (4.1 g, 38 mmol) was added and the mixture was stirred for 20 min at 40°C. Triphenyl phosphite (9.5 ml, 36 mmol) was added dropwise to the resulting white emulsion and the reaction mixture was stirred for 4 h at 100°C. After further reaction at 20–25°C for 12 h, 25 ml water were added, resulting in a white oil. Addition of 25 ml methanol afforded 3.9 g (62%) of white crystals with mp 238°C (from nitromethane). ^{1}H-NMR ($CDCl_3$, TMS) $\delta = 2.59$ (s, 6H, CH_3), 7.00 (d, 2H, m′-PyH), 7.73 (t, 2H, p′-PyH), 8.16 (t, 1H, p-PyH), 8.35 (d, 2H, m-PyH), 8.50 (d, 2H, m′-PyH), 11.24 (s, 2H, NH). Anal. Calcd. for $C_{19}H_{17}N_5O_2$: C, 65.69; H, 4.93; N, 20.16. Found: C, 65.72; H, 4.90; N, 20.20%. MS [M + H]: 348.1411. Calcd. for $C_{19}H_{17}N_5O_2$, [M + H]: 348.386.

N,N′-Diphenylpyridine-2,6-dicarboxamide (2)

Compound **2** was prepared in accordance with a previously described procedure [28]. ^{1}H-NMR (DMSO-d_6, TMS) $\delta = 7.17–7.22$ (m, 2H, PhH), 7.41–7.47 (m, 4H, PhH), 7.89–7.93 (m, 4H, PhH), 8.30 (m, 1H, p-PyH), 8.40 (d, 2H, m-Py-H), 11.03 (s, 2H, NH).

Co^{III} Complex of 1

Compound **1** (0.236 g, 0.68 mmol) was dissolved in freshly distilled *N,N′*-dimethylformamide (DMF; 5 ml) under argon and reacted with 55 mg (1.38 mmol) solid NaH while stirring for 30 min. This solution was combined with a liquid mixture prepared also under argon from $N(C_4H_9)_4ClO_4$ (0.116 g, 0.34 mmol) and $Co(ClO_4)_2 \times nH_2O$ (0.087 g) in 10 ml DMF and stirred for 2 h. Exposure to air (overnight) resulted in a color change from blue–violet to green–brown. The reaction mixture was filtered and the solvent was evaporated from the filtrate *in vacuo*. 10 ml acetonitrile were added to the resulting residue and after slow evaporation, dark green crystals of the complex were obtained. The sample for elemental analysis was additionally dried *in vacuo*. Yield 17.1%. Anal. Calcd. for $C_{76}H_{60}N_{20}O_8Co_2Na_3 \times ClO_4$: C, 54.72; H, 3.63; N, 16.79. Found: C, 54.58; H, 3.86; N, 16.90%.

Co^{III} Complex of 2

In a similar procedure as for the Co^{III} complex of **1**, $Co^{III}(\mathbf{1})_2$, two solutions containing $Co(ClO_4)_2 \times nH_2O$ (0.087 g) and $N(C_4H_9)_4ClO_4$ (0.116 g, 0.34 mmol) in 10 ml freshly distilled DMF, as well as **2** (0.215 g, 0.68 mmol) and solid NaH (0.033 g, 1.38 mmol) in 5 ml DMF (the latter mixture stirred previously for 30 min at room temperature under argon), were reacted under a normal atmosphere of air overnight. After filtration of the reaction mixture, the filtrate was evaporated *in vacuo*. The residue was diluted with 10 ml acetonitrile and yielded green crystals of the complex after slow evaporation (24.3%). Anal. Calcd. for $C_{76}H_{52}N_{12}O_8Co_2Na_2 \times 5H_2O$: C, 60.24; H, 3.46; N, 11.09. Found: C, 60.44; H, 3.20; N, 11.28%.

RESULTS AND DISCUSSION

The structure of ligand **1** containing three pyridine moieties is depicted in Fig. 1 and all the relevant crystal data and details of crystal structure determinations are given in Table I. The molecule contains a two-fold axis coinciding with that of the space group $C2/c$. The distances N(1)–C(1) = N(1)–C(1′) = 1.333 Å, N(3)–C(5) = 1.333 Å, and N(3)–C(9) = 1.344 Å are comparable with normal

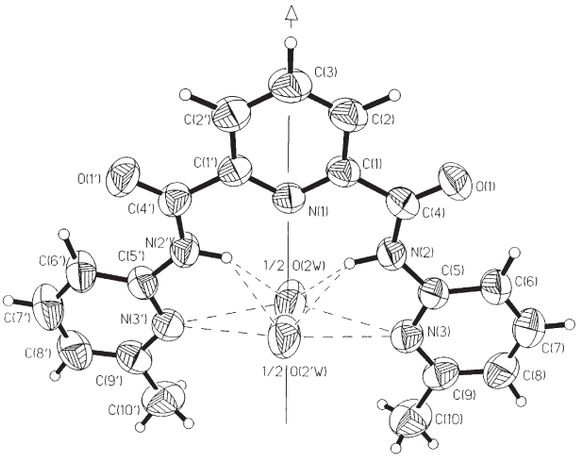

FIGURE 1 View of the molecular structure of **1** drawn at 50% probability level. The molecule contains a 2-fold axis coinciding with that of the space group $C2/c$.

C–N bonds in aromatic systems. The bond angles at N(1) and N(3) are 117.6° and 118.6°. As would be expected from a theoretical point of view, these values are significantly smaller than 120°. The distance N(2)–C(4) equals 1.352 Å and corresponds to such bond lengths in peptide bonds. The distances between C(1) and C(4) = 1.507 Å as well as N(2) and C(5) = 1.408 Å, however, indicate single bonds, allowing a pronounced degree of rotational freedom. Nevertheless, the whole molecule is planar, an advantageous predisposition with respect to complex formation [35]. Whereas in the case of **1**, this planarity is reflected by the torsion angles of bonds C(1)–C(4), C(4)–N(2), and N(2)–C(5) with absolute values of 0.7°, 4.7°, and 1.8°, the picture is different for **2**. For this ligand, Malone *et al.* found corresponding torsion angles between 6° and 28° [32]. As shown in Fig. 1, ligand **1** is intramolecularly connected via hydrogen bonds with one additional water molecule, the position of which is split into one above and one below the molecular plane. The N···O distances are between 2.78 and 2.97 Å, suggesting that these hydrogen bonds most probably stabilize the planar structure. Apparently, water-assisted stabilization is favored as compared to direct intra-ligand hydrogen bonding from N(2)H···N(1) as found for **2** [32].

Figure 2 shows a part of the very complex crystal structure of **3**, containing two symmetry-independent $Co^{III}(\mathbf{1})_2$ complexes, three Na^+ ions, a perchlorate anion, and many water molecules of which 16 could be located. The sodium ions are coordinated by water molecules and carbonyl oxygens, forming irregular polyhedra. The Na–O distances are between 2.11 and 2.83 Å. The shortest Na–Na distances are Na(1)–Na(3) = 3.98 and Na(2)–Na(3) = 4.06 Å. The sodium–oxygen polyhedra connect the $Co^{III}(\mathbf{1})_2$ complexes in such a way that infinite double chains

TABLE I Crystal data and details of structure determination for **1**, **3**, and **4**

	1	**3**	**4**
Empirical formula	$C_{19}H_{17}N_5O_2 \times H_2O$	$C_{76}H_{60}N_{20}O_8Co_2 \times ClO_4 \times 3\ Na \times 16\ H_2O$	$C_{76}H_{52}N_{12}O_8Co_2 \times 2\ Na \times 5\ H_2O$
Formula weight/g mol^{-1}	365.39	1955.98	1515.22
Temperature/K	293(2)	293(2)	293(2)
Wavelength (Mo-Kα)/Å	0.71073	0.71073	0.71073
Crystal system	Monoclinic	Orthorhombic	Monoclinic
Space group	$C2/c$	$P2_12_12_1$	$P2_1/n$
Unit cell dimensions/Å	$a = 13.614(3)$	$a = 12.325(8)$	$a = 20.321(9)$
	$b = 11.525(2)$	$b = 16.248(10)$	$b = 16.429(7)$
	$c = 12.727(3)$	$c = 48.570(30)$	$c = 22.481(9)$
	$\beta = 113.544(4)°$		$\beta = 99.625(8)°$
Volume/Å^3	1830.7(6)	9726(11)	7400(5)
Calculated density/Mg m^{-3}	1.326	1.336	1.360
No. of formula units in the unit cell	4	4	4
Absorption coefficient/mm^{-1}	0.093	0.464	0.531
Absorption correction	Semi-empirical	Semi-empirical	None
Max. and min. transmission	0.323 and 0.572	0.219 and 0.265	–
$F(000)$	800	4064	3128
Crystal size/mm	$0.90 \times 0.28 \times 0.20$	$0.25 \times 0.20 \times 0.13$	$0.55 \times 0.25 \times 0.18$
Θ range of data coll./deg	2.4–28.0	0.8–24.0	1.25–24.00
Collected reflections	5334	36454	33244
Independent reflections	2159 ($R_{int} = 0.056$)	14918 ($R_{int} = 0.058$)	11599 ($R_{int} = 0.036$)
Final R-indices [$I > 2\sigma(I)$]	$R1 = 0.0563$	$R1 = 0.1180$	$R1 = 0.0616$
	$wR2 = 0.1833$	$wR2 = 0.2900$	$wR2 = 0.2359$

are formed along the x-direction of the crystal. The crystal structure of **4** is depicted in Fig. 3. This complex also contains two symmetry independent $Co^{III}(\mathbf{2})_2$ complexes, however, the structural features are completed by two Na^+ ions and five water molecules. Each Na^+ is coordinated by three water molecules and two carbonyl oxygens, three of which act as a bridge between Na(1) and Na(2) (see Fig. 3). These features entail a rather short sodium–sodium distance of 3.00 Å as well as the formation of a Na_2O_7 polyhedron with Na–O distances between 2.16 and 2.54 Å. In contrast to **3**, only dimers exist in the crystal structure of **4**, i.e., two symmetry independent $Co^{III}(\mathbf{2})_2$ complexes that are connected by a Na_2O_7 polyhedron. The bond distances and angles of the complexes are given in Table II. As can be derived from Figs. 2 and 3, each cobalt atom is coordinated by four deprotonated amido nitrogens

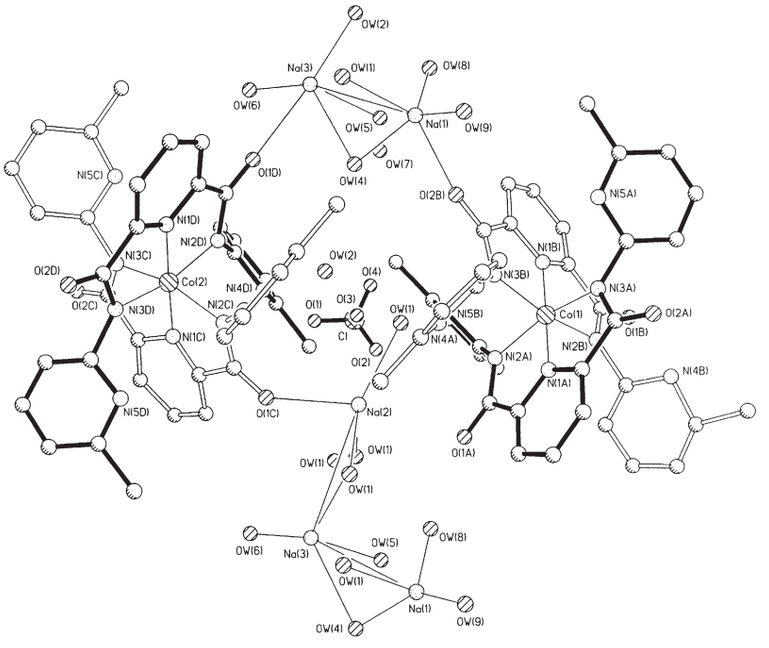

FIGURE 2 Illustration of two symmetry-independent $Co^{III}(\mathbf{1})_2$ complexes in the crystal structure of **3** and their connection by ClO_4^- and Na^+ ions as well as water molecules. Some water molecules are omitted for clarity.

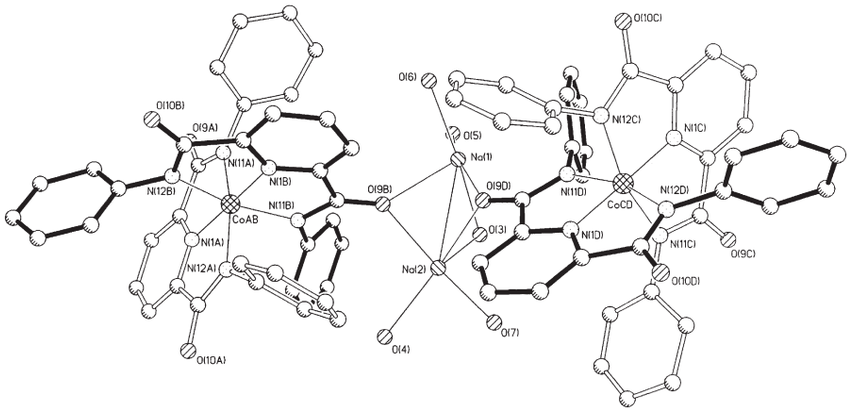

FIGURE 3 Crystal structure of **4** containing two symmetry-independent $Co^{III}(\mathbf{2})_2$ complexes, two Na^+ ions, and five water molecules.

in the equatorial plane [N(2A), N(3A), N(2B), and N(3B) as well as N(2C), N(3C), N(2D), and N(3D), respectively], assisted by the two nitrogen atoms of the central pyridyl group [N(1A), N(1B) and N(1C), N(1D)] in the axial positions.

The geometry of the CoN_6 coordination polyhedra is octahedral but notably compressed. The average value of the axial Co–N(1) bonds amounts to 1.844 Å. This unusually short distance is in good agreement with corresponding values found by Ray *et al.* in Fe^{III} and Co^{III} complexes of **2** [28]. Furthermore, in the case of **3** with a slightly unsymmetrical coordination of the two ligands to each central ion, this bond is even shorter for the tightly bound pyridino nitrogen atoms N(1A) and N(1C), equalling 1.800 and 1.808 Å, respectively. In all the complexes of **3** and **4**, the average value of the equatorial Co–N_{amido} bonds is 1.964 Å. As shown in Table II, significant deviations from 90° are found for the bond angles at the cobalt atom, most probably caused by the bulkiness and adopted geometry of the ligand molecules.

As mentioned above, the molecule of the free ligand **1** is planar. In the complexes of both structures, however, only the central pyridine-2,6-dicarboxamide fragments are planar. All methylpyridyl groups in **3** and all phenyl groups in **4** are considerably twisted out of the plane, the torsion angles of the N(2)–C(7) and N(3)–C(14) bonds ranging from 57.2 to 85.2°. Apparently, steric hindrance of the branched ligands within the complex causes the strong deviation from planarity. An interesting feature for **3** is the fact that the resulting ligand conformation in combination with

TABLE II Selected bond lengths (Å) and angles (deg) of the two symmetry independent coordination spheres of **3** and **4**

	3		**4**	
	[Co1, LA, LB]	**[Co2, LC, LD]**	**[Co1, LA, LB]**	**[Co2, LC, LD]**
Co(1,2)–N(1A,1C)*	1.800(9)	1.808(11)	1.845(6)	1.850(6)
Co(1,2)–N(1B,1D)	1.888(10)	1.869(9)	1.842(6)	1.849(6)
Co(1,2)–N(2A,2C)	2.006(10)	2.010(9)	1.937(6)	1.948(5)
Co(1,2)–N(2B,2D)	2.010(10)	1.956(9)	1.965(6)	1.962(5)
Co(1,2)–N(3A,3C)	1.932(10)	1.951(10)	1.954(6)	1.956(6)
Co(1,2)–N(3B,3D)	1.940(9)	1.978(9)	1.946(6)	1.965(5)
N(1A,1C)–Co(1,2)–N(1B,1D)	176.9(5)	177.7(5)	177.7(3)	179.0(2)
N(2A,2C)–Co(1,2)–N(3A,3C)	163.0(4)	161.7(5)	164.1(3)	163.6(3)
N(2B,2D)–Co(1,2)–N(3B,3D)	164.5(4)	164.0(4)	163.9(2)	162.7(2)
N(1A,1C)–Co(1,2)–N(2A,2C)	80.7(4)	79.5(4)	82.3(3)	81.9(3)
N(1A,1C)–Co(1,2)–N(2B,2D)	96.3(4)	96.3(4)	100.2(2)	98.2(2)
N(1A,1C)–Co(1,2)–N(3A,3C)	82.3(4)	82.3(5)	81.8(2)	81.7(3)
N(1A,1C)–Co(1,2)–N(3B,3D)	99.1(4)	98.2(5)	95.9(2)	99.1(2)
N(1B,1D)–Co(1,2)–N(2A,2C)	96.8(4)	98.1(4)	98.9(3)	99.1(2)
N(1B,1D)–Co(1,2)–N(3A,3C)	100.2(5)	100.1(4)	96.9(2)	97.4(2)
N(1B,1D)–Co(1,2)–N(3B,3D)	82.7(4)	81.8(4)	82.2(3)	81.2(3)
N(2A,2C)–Co(1,2)–N(2B,2D)	88.9(4)	92.8(4)	90.9(2)	91.5(2)
N(3A,3C)–Co(1,2)–N(3B,3D)	89.9(4)	90.7(4)	90.8(2)	91.6(2)
Co(1,2)—N(4A,4C)	3.501(10)	3.615(10)		
Co(1,2)—N(4B,4D)	3.721(11)	3.500(11)		
Co(1,2)—N(5A,5C)	3.530(10)	3.490(10)		
Co(1,2)—N(5B,5D)	3.637(10)	3.587(10)		

*Read as Co(1)–N(1A) = 1.800, Co(2)–N(1C) = 1.808.

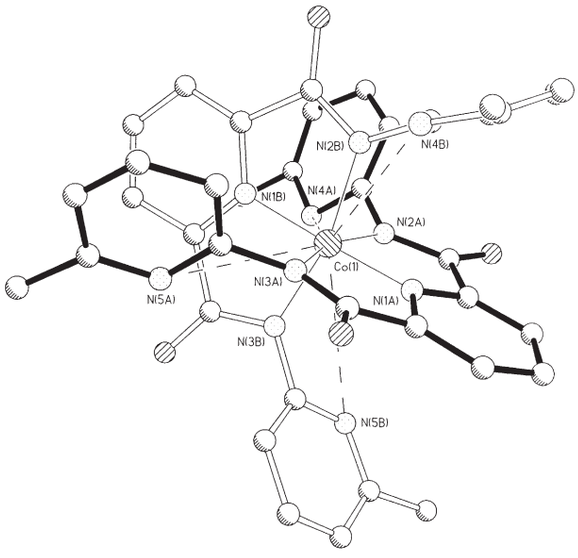

FIGURE 4 Single complex of the crystal structure of **3** showing the second-order Co–N bonds as dashed lines.

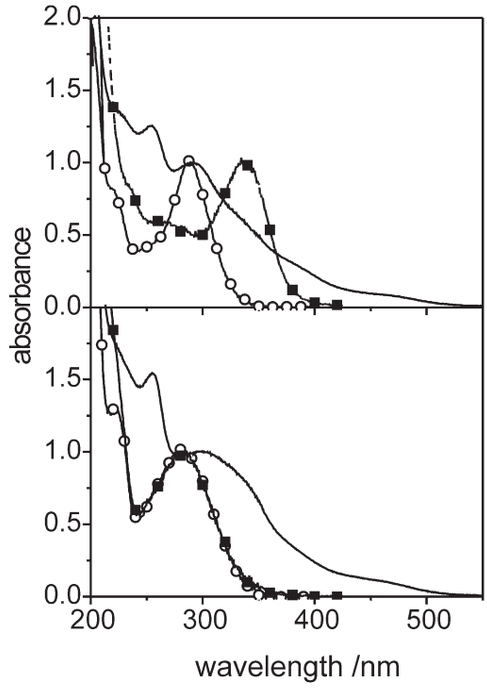

FIGURE 5 Upper part: absorption spectra of **1** (circles), Co^{II}–**1** (squares), and **3** (full line) in acetonitrile. Lower part: absorption spectra of **2** in the absence (circles) and presence (squares) of 500 μM Co^{II} (the spectra are virtually identical) as well as **4** (full line) in acetonitrile.

the two terminal pyridyl groups leads to long-range interactions. These interactions are manifested by the formation of second-order bonds between Co and the respective nitrogen donor atoms N(4) and N(5). Figure 4 illustrates this second sphere coordination with bond lengths from 3.50 to 3.72 Å.

The absorption spectra of the complexes **3** and **4** dissolved in acetonitrile are shown in Fig. 5, along with the absorption spectra of the free ligands and their Co^{II} complexes as obtained by titrating **1** and **2** with a solution of $Co(ClO_4)_2$ in the same solvent. The spectra of **3** and **4** are qualitatively similar with intense ligand-centered transitions below 400 nm and ligand-to-metal charge-transfer (LMCT) bands at ca. 450 nm, in accordance with results reported by Ray *et al.* [28]. In contrast, the titration experiments in solution reveal pronounced differences. In the case of Co^{II}, complexation occurs only for the ligand containing three pyridyl moieties and essentially no changes are observed for the diphenyl analogue **2**. Moreover, as is evident from the data on all the other heavy and transition metal ions studied in the solution-based experiments, the coordination ability of **1** is generally much stronger towards these species (see Table III). Besides the oxophilic main group metal ions Ca^{II} and Na^{I}, which were used for control experiments, only Mn^{II} and Ag^{I} showed no interaction with **1** up to a 100-fold excess, i.e., 500 μM of metal ion. The latter observation is conceivable with the generally weaker binding ability of these ions [36] and, most probably, in the case of Ag^{I} with its strong solvation in acetonitrile [37]. The cations that are bound by **1** can be classified into two groups. Co^{II}, Ni^{II}, Cu^{II}, and Zn^{II} induce very similar bathochromic shifts of ca. 45 nm. The titrations yield sharp isosbestic points and data analysis suggests that in the case of Co^{II}, Ni^{II}, Cu^{II}, and Zn^{II} complexes of 1:1 stoichiometry are formed with $\log K_S$ of 5.0, 4.5, 5.0, and 6.1, respectively. For Cu^{II}, a slight deviation from linearity is observed in the Hill plots, so we assume that mixed formation of two different complexes occurs to some extent. On the other hand, binding to Fe^{III}, Fe^{II}, Hg^{II}, and Pb^{II} mainly leads to red-shifts of only 20 nm. Furthermore, during a titration with the latter three divalent cations, several isosbestic points are found as a function of cation concentration.

TABLE III Absorption maxima (nm) of **1** and **2** in the absence and presence of cations in acetonitrile at 298 K*

	Free	Co^{II}	Ni^{II}	Cu^{II}	Zn^{II}	Fe^{III}	Fe^{II}	Hg^{II}	Pb^{II}	H^{+}
1	289	337	337	331	332	309	308, 333†	311, 348†	311, 348‡	308
2	282	–¶	–	297	(285)§	–	–	–	312	347

* No spectroscopic changes occur for up to 500 μM Mn^{II} and Ag^{I} as well as 50 mM Na^{I} and Ca^{II}. † Red-shifted band appears only at a metal ion-to-ligand ratio >1 and increases with increasing ion concentration. ‡ Both bands appear and increase almost simultaneously at a metal ion-to-ligand ratio >1. ¶ No spectroscopic changes occur for up to 500 μM metal ion. § Observable only at a high metal ion concentration of 200 μM.

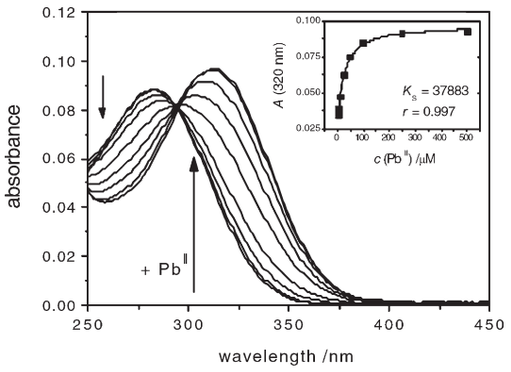

FIGURE 6 Spectrophotometric titration spectra of **2** and $Pb(ClO_4)$ in acetonitrile. Inset: example of a fit of the increase of the absorbance at 320 nm.

Generally, the appearance of a band at 310 nm at equimolar ratios of ion and ligand is followed by the build-up of a further red-shifted band at >330 nm at higher cation excess. Presumably, the coordination mode changes during the titration or several different complexes are formed at a higher ion excess.

The behavior of **1** is contrasted by that of **2** in such a way that the bisamidopyridine unit alone is not a very powerful chelating agent in solution. Besides very weak shifts in the presence of Cu^{II} and Zn^{II}, only Pb^{II} is able to coordinate to **2** in acetonitrile (Fig. 6). The corresponding complexation features are the appearance of a new band at 312 nm, a spectroscopically detectable complex stoichiometry of 1:1, and a log $K_S = 4.6$. Apparently, the additional donor atoms at the terminal aromatic substituents are important for the improved metal ion response of **1**. Concerning protonation, **1** is readily protonated at moderate concentrations of dilute perchloric acid (apparent $pK_a = 4.30$ for a titration of **1** with $HClO_4$ in acetonitrile). The shifts found in absorption are qualitatively identical to those observed, for instance, for Fe^{III} and Hg^{II} at low concentrations. The molar absorptivity of the new species is considerably increased, suggesting enhanced charge-transfer interaction. In contrast, the apparent $pK_a = 2.19$ of **2** is considerably lower and more concentrated perchloric acid is necessary to obtain a spectroscopic proton-response from this receptor.

In order to obtain some information on the nature of the complexes formed in solution, it is helpful to compare the results obtained for closed- and open-shell as well as more (e.g., Zn^{II}) and less aminophilic (e.g., Pb^{II}) metal ions and **1**, the protonation behavior of both ligands, and the geometric and molecular orbital features as derived from quantum chemical calculations. Before embarking on a discussion, the most important theoretical results will be briefly described.

To verify published results of **2**, we performed calculations at the AM1 level employing previously described software packages and procedures [30] and followed the routine adopted by Malone *et al*. in their respective theoretical treatment of the phenyl analogue **2** [32]. In principle, we could reproduce their results, i.e., the most stable conformation is the *syn–syn* structure with torsion angles $\alpha = \alpha' = 34°$ and a calculated heat of formation of 28.11 kcal mol^{-1} [α = N(1)–C(1)–C(4)–N(2), α' = N(1)–C(1′)–C(4′)–N(2′) (Scheme 2); for atom labeling, see Fig. 1]. The only difference in our study was that with the convergence criteria chosen here, both other starting conformations (*syn–anti* and *anti–anti*) also fully relaxed to the *syn–syn* conformation. For **1**, the basic results are comparable to those of **2**. Again, all the starting conformations relax to *syn–syn*, with torsion angles of ca. 30°. Only a *syn–syn* conformation with $\alpha = 27°$ and $\alpha' = -24°$ was also found to represent a minimum, although less preferred by 0.2 kcal mol^{-1}. Moreover, from the possible conformations at the terminal groups, all the starting geometries relax to "N(3)O(1)–*anti*" (Scheme 2). Concerning electronic transitions, for both ligands, HOMO and LUMO are localized on different parts of the molecule, i.e., the highest occupied molecular orbital on the Ar–NH (with Ar = methylpyridyl or phenyl) and the lowest unoccupied MO on the CO–pyridine–CO fragment.

Calculating the protonated structures reveals some important changes. For **2**-H^+ with a protonated pyridine moiety, the *anti–anti* conformation is now the most preferred one. Although in this case, the *syn–anti* and the *syn–syn* geometries also converged they were found to be less stable by 1.1 and 2.9 kcal mol^{-1}. However, the frontier molecular

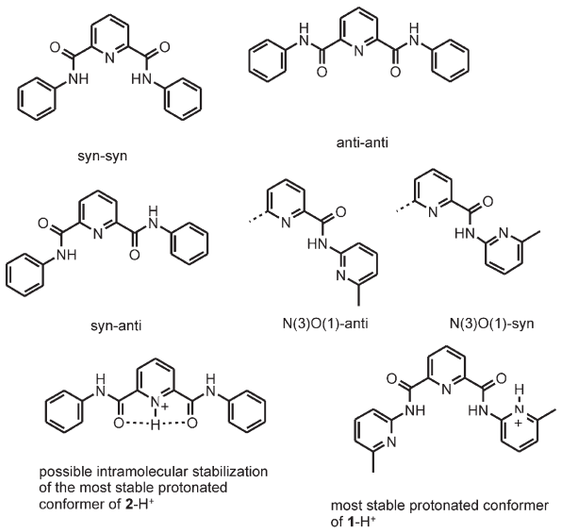

SCHEME 2 Different possible conformers of **1** and **2** as discussed in the text.

orbitals remain localized on the respective fragments as in the unprotonated molecule and the twist between the molecular subunits is also not very much altered ($\alpha = \alpha' = -143°$). The data suggest that the change from *syn–syn* to *anti–anti* might be facilitated by hydrogen bonding between the proton at the pyridino nitrogen atom N(1) and the carbonyl oxygens, with H···O distances of ca. 2.5 Å. In the case of **1**, however, the most stable species is the N(3)-protonated *syn–syn* conformation, again with possible internal stabilization (Scheme 2). The complementary N(3)O(1)–*anti* structure is 6.4 kcal mol^{-1} less preferred and all the species with a protonated central pyridine moiety are more than 20 kcal mol^{-1} less stable. (Note that the second protonation occurs at $pK^{app} < 0$.) This is consistent with the higher charge density found for N(3) than for N(1), i.e., net charges of -0.183 and -0.116, respectively. Accordingly, for N(3)-protonated **1**–H$^+$, the HOMO is still localized on the unprotonated terminal pyridine ring, but the LUMO is found on the other terminal, protonated group.

In consequence, such changes involve a dramatic reconfiguration of the intramolecular charge-transfer which should be also reflected in the electronic transitions. For the most stable conformers of **1** and **2**, the lowest spin-allowed transitions with appreciable oscillator strength are found at ca. 300 nm. In the N(1)-protonated ligands, these transitions are shifted to considerably lower energies and show increased oscillator strengths. For N(3)-protonated **1**–H$^+$, the respective transitions are also oscillator strong, however, they are found at intermediate energies.

Returning to the discussion of the complexation-induced features, a comparison of the absorption bands of the complexes of **1** with open- and closed-shell metal ions reveals no significant differences. This suggests that no LMCT (or MLCT) transitions are involved in solution for the metal-bound neutral ligand and mainly the electrostatic polarization induced by the metal ion accounts for the bathochromic shifts [38]. The comparatively weak change in molar extinction coefficients upon metal ion binding supports the assumption that the transitions remain ligand-centered. Thus, on the basis of the similarity of the spectral protonation data of **2** (at 347 nm) and the complexes of **1** with more aminophilic metal ions (at ca. 335 nm), we tentatively assign the bathochromically absorbing complex species to coordination to the central pyridine ring or N(1), probably stabilized by one of the second terminal pyridine moieties. This is supported by the theoretical results for N(3)- and N(1)-protonated **1**. Presumably, the less aminophilic cations prefer coordination involving N(3), also with a possible support by the second terminal pyridine group or by formation of a six-membered ring chelate [39] in a N(3)O(1)–*syn* conformation (Scheme 2). Thus, we assume that the similarity of the absorption band maxima of 2-Pb^{II} and N(3)-protonated **1** is only coincidential and arises from weaker interaction of the lead ion with the nitrogen atom.

CONCLUSION

In summary, the investigation and characterization of the complexation behavior of a bisamidopyridine-type receptor with two additional donor groups stressed the potential such ligands can have for various aspects of coordination chemistry. Besides allowing the stabilization of complexes with carboxamido–metal ion bonds, the presence of different coordinative substructures offers the possibility to address different donor atoms or auxochromic fragments with different cations. Whereas the first feature might yield a better stabilization of higher oxidation states of certain transition metal ions, the second fact should open up new ways in the design of metal ion-responsive molecular sensors. Finally, the importance of amido group deprotonation for efficient complex formation of the basic bisamidopyridine carboxamide moiety is strikingly evident from the similarity of **3** and **4** on the one hand and the pronounced difference in metal ion responsivity of **1** and **2** in solution on the other hand. Unfortunately, up to now, we have not yet been able to obtain suitable crystals for X-ray analysis of the Co$^{II/III}$ or Fe$^{II/III}$ complexes of **1** with intact amido groups, to get a picture of the coordination mode of these species.

Acknowledgements

Financial support by BAM-MOE and the Deutsche Forschungsgemeinschaft is gratefully acknowledged.

References

[1] Kobayashi, M.; Shimizu, S. *Nat. Biotechnol.* **1998**, *16*, 733.
[2] Mascharak, P. K. *Coord. Chem. Rev.* **2002**, *225*, 201.
[3] Ray, M.; Mukherjee, R.; Richardson, J. F.; Buchanan, R. M. *J. Chem. Soc., Dalton Trans.* **1993**, 2451.
[4] Marlin, D. S.; Mascharak, P. K. *Chem. Soc. Rev.* **2000**, *29*, 69.
[5] Eide, D. J. *Adv. Microb. Physiol.* **2000**, *43*, 1.
[6] Arii, H.; Nagatomo, S.; Kitagawa, T.; Miwa, T.; Jitsukawa, K.; Einaga, H.; Masuda, H. *J. Inorg. Biochem.* **2000**, *82*, 153.
[7] Wisner, J. A.; Beer, P. D.; Drew, M. G. B. *Angew. Chem., Int. Ed.* **2001**, *40*, 3606.
[8] Szumna, A.; Jurczak, J. *Eur. J. Org. Chem.* **2001**, 4031.
[9] Fitzmaurice, R. J.; Kyne, G. M.; Douhert, D.; Kilburn, J. D. *J. Chem. Soc., Perkin Trans. 1* **2002**, 841.
[10] Mazik, M.; Bandmann, H.; Sicking, W. *Angew. Chem., Int. Ed.* **2000**, *39*, 551.
[11] Mazik, M.; Sicking, W. *Chem. Eur. J.* **2001**, *7*, 664.
[12] You, J.-S.; Yu, X.-Q.; Zhang, G.-L.; Xiang, Q.-X.; Lan, J.-B.; Xie, R.-G. *Chem. Commun.* **2001**, 1816.

[13] Bourgel, C.; Boyd, A. S. F.; Cooke, G.; Augier de Cremiers, H.; Duclairoir, F. M. A.; Rotello, V. M. *Chem. Commun.* **2001**, 1954.
[14] Tucker, J. H. R.; Collinson, S. R. *Chem. Soc. Rev.* **2002**, *31*, 147.
[15] Pickaert, G.; Douce, L.; Ziessel, R.; Guillon, D. *Chem. Commun.* **2002**, 1584.
[16] Hennrich, G.; Anslyn, E. V. *Chem. Eur. J.* **2002**, *8*, 2218.
[17] Chavez, F. A.; Olmstead, M. M.; Mascharak, P. K. *Inorg. Chem.* **1996**, *35*, 1410.
[18] Marlin, D. S.; Olmstead, M. M.; Mascharak, P. K. *Inorg. Chim. Acta.* **2000**, *297*, 106.
[19] Rat, M.; Alves de Sousa, R.; Vaissermann, J.; Leduc, P.; Mansuy, D.; Artaud, I. *J. Inorg. Biochem.* **2001**, *84*, 207.
[20] Tyler, L. A.; Olmstead, M. M.; Mascharak, P. K. *Inorg. Chim. Acta.* **2001**, *321*, 135.
[21] Rettig, W.; Rurack, K.; Sczepan, M. In *New Trends in Fluorescence Spectroscopy: Applications to Chemical and Life Sciences*; Valeur, B., Brochon, J. C., Eds.; Springer: Berlin, 2001; p 125.
[22] Rurack, K.; Resch-Genger, U. *Chem. Soc. Rev.* **2002**, *31*, 116.
[23] Rurack, K.; Resch-Genger, U.; Bricks, J. L.; Spieles, M. *Chem. Commun.* **2000**, 2103.
[24] Kollmannsberger, M.; Rurack, K.; Resch-Genger, U.; Rettig, W.; Daub, J. *Chem. Phys. Lett.* **2000**, *329*, 363.
[25] Rurack, K. *Spectrochim. Acta, Part A* **2001**, *57*, 2161.
[26] Bricks, J. L.; Slominskii, J. L.; Kudinova, M. A.; Tolmachev, A. I.; Rurack, K.; Resch-Genger, U.; Rettig, W. *J. Photochem. Photobiol., A. Chem.* **2000**, *132*, 193.
[27] Singha, N. C.; Sathyanarayana, D. N. *J. Mol. Struct.* **1997**, *403*, 123.
[28] Ray, M.; Ghosh, D.; Shirin, Z.; Mukherjee, R. *Inorg. Chem.* **1997**, *36*, 3568.
[29] Redmore, S. M.; Rickard, C. E. F.; Webb, S. J.; Wright, L. J. *Inorg. Chem.* **1997**, *36*, 4743.
[30] Rurack, K.; Bricks, J. L.; Schulz, B.; Maus, M.; Reck, G.; Resch-Genger, U. *J. Phys. Chem. A* **2000**, *104*, 6171.
[31] Sheldrick, G., SHELX-97, University of Göttingen, 1997
[32] Malone, J. F.; Murray, C. M.; Dolan, G. M.; Docherty, R.; Lavery, A. J. *Chem. Mater.* **1997**, *9*, 2983.
[33] Fery-Forgues, S.; Le Bris, M.-T.; Guetté, J.-P.; Valeur, B. *J. Phys. Chem.* **1988**, *92*, 6233.
[34] Bourson, J.; Pouget, J.; Valeur, B. *J. Phys. Chem.* **1993**, *97*, 4552.
[35] Rowland, J. M.; Thornton, M. L.; Olmstead, M. M.; Mascharak, P. K. *Inorg. Chem.* **2001**, *40*, 1069.
[36] Irving, H.; Williams, R. J. P. *Nature* **1948**, *162*, 746.
[37] Cox, B. G.; Stroka, J.; Firman, P.; Schneider, I.; Schneider, H. *Aust. J. Chem.* **1983**, *36*, 2133.
[38] Schläfer, H. L. *Z. Phys. Chem., Neue Folge* **1956**, *8*, 373.
[39] Rurack, K.; Radeglia, R. *Eur. J. Inorg. Chem.* **2000**, 2271.